Dynamic Disorder-Driven Substrate Inhibition and Bistability in a Simple Enzymatic Reaction

Srabanti Chaudhury and Oleg A. Igoshin*

Department of Bioengineering, Rice University, Houston, Texas 77005

Received: June 5, 2009

Conformations and catalytic rates of enzymes (biological catalysts) fluctuate over a wide range of time scales. Recent experimental and theoretical investigations demonstrated case studies where the enzymatic catalysis rate follows the Michaelis−Menten (MM) rate law despite molecular fluctuations. In this paper, we investigate deviations from MM law and their effects on the dynamical behavior of the enzymatic network. We consider a simple kinetic scheme for a single substrate enzymatic reaction in which the product release step is treated explicitly. We examine how conformational fluctuations affect the underlying rate law in the quasi-static limit when conformational dynamics is very slow in one of the states. Our numerical results and analytically solvable model indicate that slow conformational fluctuations of the enzyme−substrate complex lead to non-MM behavior, substrate inhibition, and possible bistability of the reaction network.

1. Introduction

Enzymes (protein catalysts) play an important role in controlling the flux of biochemical reaction networks. The classic Michaelis−Menten (MM) mechanism, proposed in 1913, provided a highly satisfactory description of the catalytic activity of an enzyme.[1,2] In its simplest formulation, a substrate S combines reversibly with an enzyme E to form an ES complex, which undergoes catalytic transformation, immediately followed by the release of the product P and the regeneration of the original enzyme

$$\mathrm{E} + \mathrm{S} \underset{k_{21}}{\overset{k_{12}}{\rightleftharpoons}} \mathrm{ES} \xrightarrow{k_{23}} \mathrm{E} + \mathrm{P} \tag{1}$$

Under the steady state conditions, the rate of product formation, V, is given by

$$V = \frac{V_{\max}[\mathrm{S}]}{[\mathrm{S}] + K_{\mathrm{M}}} \tag{2}$$

where square brackets denote concentration and the kinetic parameters are given by MM constant $K_{\mathrm{M}} = (k_{21} + k_{23})/k_{12}$ and maximal rate $V_{\max} = k_{23}[\mathrm{E}]_{\mathrm{T}}$ proportional to total enzyme concentration.

Conformational flexibility and dynamics of enzymes play important roles in their functional properties. Fluctuations in the protein structure can bring changes in the substrate/product affinities and catalytic properties of enzymes.[3−5] The importance of conformational dynamics has been realized for quite some time and has been widely studied in the context of allosteric regulation—propagation of the ligand binding effect to a distant catalytic site.[6] In recent years, a large number of different tools have been developed for probing the conformations of enzymes during catalysis. Single-molecule[7−9] and NMR[10] experiments suggest that conformational fluctuations occur over vast distribution of time scales: from milliseconds to 100 s. Interestingly, single molecule measurements of β-galactosidase enzymatic kinetics show that the rate of the catalytic reaction fluctuates over a similar range of time scales (10^{-4}−10 s),[11] a phenomenon termed dynamic disorder.[12] These experimental observations have inspired several theoretical studies[13−18] on the effects of conformational dynamics on the kinetics of single enzymatic reactions. The results of some of these theoretical studies indicate that in general the steady state kinetics of a fluctuating enzyme are non-MM[14,15] but depict several limiting cases in which the MM equation is obeyed even for single-molecule reactions. The limits considered include the quasi-equilibrium limit when the catalytic transition is slow so that conformational dynamics and binding-dissociation reactions equilibrate before the reaction occurs. Another important limit motivated by experimental work is the quasi-static limit in which fluctuations in any one of the conformational states (E or ES) is very slow. In this paper, we aim to show that for the kinetic scheme with more than two enzyme states, slow conformation dynamics of one can lead to quantitative and qualitative violations of the MM rate law. As a result, dynamic disorder manifests itself in an excess substrate inhibition effect: increases in substrate concentration decrease the catalytic turnover rate.

2. Theoretical Formalism

We consider a generalized MM reaction scheme in which a complex between the enzyme and product, and the subsequent product release reaction, is explicitly considered:

$$\mathrm{E} + \mathrm{S} \underset{k_{21}}{\overset{k_{12}}{\rightleftharpoons}} \mathrm{ES} \underset{k_{32}}{\overset{k_{23}}{\rightleftharpoons}} \mathrm{EP} \xrightarrow{k_{31}} \mathrm{E} + \mathrm{P} \tag{3}$$

Despite the presence of an additional state, conventional chemical kinetics still result in the MM law (eq 2) with constants

* Corresponding author. E-mail: igoshin@rice.edu. Phone: 1-713-348-5502. Fax: 1-713-348-5135.

10.1021/jp907908d CCC: $40.75
Published on Web 09/17/2009

$$V_{max} = \frac{k_{12}k_{23}k_{31}[E]_T}{k_{12}(k_{23} + k_{32} + k_{31})} \quad (4a)$$

and

$$K_M = \frac{k_{21}k_{32} + k_{21}k_{31} + k_{23}k_{31}}{k_{12}(k_{23} + k_{32} + k_{31})} \quad (4b)$$

These expressions reduce to the classical form when the product release step is fast ($k_{31} \rightarrow \infty$). We considered the case when k_{23} and k_{31} are comparable.

To investigate the effects of conformational fluctuations on the steady state kinetics of a fluctuating enzyme, we introduce a continuous conformational coordinate x, characterizing enzyme and its complexes (i.e., E, ES, and EP). For simplicity here, we treat this coordinate as one-dimensional assuming that only one of the degree of freedom is rate limiting. It is also common to assume that this conformational coordinate is perpendicular to reaction coordinates but the rates of reaction transitions (such as substrate binding and dissociation or catalysis) are functions of conformational coordinate. Alternative to this description are the discretized state models in which the conformations are discretized into several states.[13,14] Cao et al.[13] have proposed two-channel and three-channel stochastic models to study dynamic disorder caused by conformational fluctuations and show good agreement with continuous description. The discretized models are often simpler and can lead to closed-form solutions for single-molecule enzymatic kinetics. However some recent results on the measurement of the fluctuation dynamics show that the fluctuations occur on a wide spectra of time scales[9,11] indicating a possible continuum of conformation states (rather than a few discrete conformations). As a result, it has been suggested that a continuous treatment of the conformational coordinate with a Smoluchowski−Fokker−Plank equation[19,20] is a more reasonable description than a few different conformational states. Therefore, following refs 16 and 21 we chose to describe the dynamics of the enzyme in the kinetic scheme (eq 3) by three coupled Smoluchowski equations:

$$L_E p_E(x) + (-k_{12}(x)[S]p_E(x) + k_{21}(x)p_{ES}(x) + k_{31}(x)p_{EP}(x)) = 0 \quad (5a)$$

$$L_{ES} p_{ES}(x) + (-k_{21}(x)p_{ES}(x) - k_{23}(x)p_{ES}(x) + k_{12}(x)[S]p_E(x) + k_{32}(x)p_{EP}(x)) = 0 \quad (5b)$$

$$L_{EP} p_{EP}(x) + (-k_{31}(x)p_{EP}(x) - k_{32}(x)p_{EP}(x) + k_{23}(x)p_{ES}(x)) = 0 \quad (5c)$$

where $p_i(x)$ (i = E, ES, EP) is the probability density of finding the enzyme at a conformational coordinate x in the state i (1 = E, 2 = ES, 3 = EP). The steady state distributions are normalized as $\int (p_E(x) + p_{ES}(x) + p_{EP}(x))\, dx = 1$. The term k_{ij} is the x dependent transition rate from state i to j and is given by

$$k_{ij}(x) = k_{ij}^0 \exp\{[U_i(x) - U_{ij}^\dagger(x)]/k_B T\} \quad (6)$$

where U_i the potential of each enzyme state and $U_{ij}^\dagger(x)$ is the transition state potential for an ij transition. This form of the reaction rates insures detailed balance is obeyed. The Smoluchowski operator L_i is given by

$$L_i = -\frac{D_i}{k_B T}\frac{\partial}{\partial x}\left(-\frac{\partial U_i(x)}{\partial x}\right) + D_i \frac{\partial^2}{\partial x^2} \quad (7)$$

where D_i is the diffusion coefficient. The average turnover rate per enzyme is obtained by integrating the product formation flux over all conformations ($v = V/[E]_T$):

$$v = \int (k_{23}(x)p_{ES}(x) - k_{32}(x)p_{EP}(x))\, dx = \int k_{31}(x)p_{EP}(x)\, dx \quad (8)$$

In general, this rate is dependent on substrate concentration but this dependence does not follow eq 2. However, MM dependence (eq 2) of reaction rate on substrate concentration will hold if the conformational dynamics are much faster than the rates of the chemical reactions—the result obtained in ref 16 and easily generalizable to the kinetic scheme including EP state (results not shown). Below we will analyze another limiting case in which MM holds for the simple scheme (eq 1) but not in the generalized scheme (eq 3) considered here.

3. Results and Discussion

3.1. Substrate Inhibition in the Quasi-Static Limit. In the quasi-static limit—when the conformational diffusion in one of the states is very slow—the theoretical formalism used in ref 16 to derive the MM rate law will not result in the MM law in our reaction scheme. Indeed, summation of eqs 5a−5c leads to

$$L_E p_E + L_{ES} p_{ES} + L_{EP} p_{EP} = 0 \quad (9)$$

In ref 16, only two conformations are considered ($p_{EP} = 0$) so that the quasi-static approximation ($L_i = 0$) in one of the states (i = E or ES) leads to equilibrium distribution of the other state, $L_j p_j = 0$ (j = ES or E, respectively). The latter condition leads to a solution proportional to the Boltzmann distribution $p_j(x) = \alpha \exp(-U_j(x)/k_B T)$ and subsequently to the MM rate law (hereafter, we will measure the potentials in the units of $k_B T$ and drop this factor). Unfortunately, this approach cannot be generalized when the kinetic scheme includes more than two enzyme states. Indeed, eliminating one of the terms in eq 9 corresponding to quasi-static limit do not necessitate equilibrium distribution in the other two states.

To investigate how the kinetic law will be affected by conformational fluctuations, we first solve eqs 5 numerically by using the Wang algorithm.[20,21] The potentials $U_i(x)$ and $U_{ij}^\dagger(x)$ are modeled as harmonic potentials:

$$U_i(x) = \frac{1}{2}\kappa_i(x - x_{0i})^2 + U_i^0 \quad (10a)$$

and

$$U_{ij}^\dagger(x) = \frac{1}{2}\kappa_{ij}(x - x_{ij}^e)^2 + U_{ij}^0 \quad (10b)$$

TABLE 1: Model Parameters for Enzyme States

	E	ES	EP
U_i^0	0	−1	−3
x_i^0	1	−0.5	0
κ_i	1	0.5	0.4

TABLE 2: Model Parameters for Transitions between Different Enzyme States

	E → ES	ES → E	ES → EP	EP → ES	EP → E	E → EP
k_{ij}^0	2	20	8	8	18	0
$U_{ij}^{0\dagger}$	0	3	6	6	3	3
x_{ij}^e	1	0.65	−0.65	−0.65	0.65	0.65
κ_{ij}	1	11.1	11.1	11.1	11.1	11.1

We chose the parameters (given in Tables 1and 2) to separate the conformations for the maximal catalytic transition (k_{23}) from those of product release step (k_{31}) (Figure 1). For simplicity $k_{12}(x)$ is chosen to be constant and $k_{21}(x)$ is computed from the detailed balance. The resulting conformation dependent rate constants are depicted in Figure 1. The parameters chosen correspond to the quasi-static condition (conformational dynamics in the ES state are slower than reaction transitions and the conformational dynamics of the other two states, E and EP, e.g. $D_{ES} \ll D_E, D_{EP}$). This is the limit that would result in MM law in the two-state model.[16] As shown in Figure 2a, the reaction rate shows non-MM behavior as the substrate concentration is increased. In fact, the parameters chosen demonstrate that the reaction rate decreases at high substrate concentration—a phenomenon known as *excess substrate inhibition*.

Excess substrate inhibition in enzymology has been extensively studied in many experiments, and several theoretical models have been proposed to explain the experimental data.[22,23] The phenomenon is also common in pharmokinetics where it is called high-dose inhibition, autoinhibition, or the Arndt−Schultz law.[23] The classical textbook mechanism of substrate inhibition[2] involves binding of a second molecule of the substrate to the allosteric site of the enzyme forming a complex SES with impaired catalytic activity.

$$\begin{aligned} &\mathrm{SE} \underset{k_{31}}{\overset{k_{13}}{\rightleftharpoons}} \mathrm{E} + \mathrm{S} \underset{k_{21}}{\overset{k_{12}}{\rightleftharpoons}} \mathrm{ES} \xrightarrow{k_{cat1}} \mathrm{E} + \mathrm{P} \\ &\mathrm{ES} + \mathrm{S} \underset{k_{42}}{\overset{k_{24}}{\rightleftharpoons}} \mathrm{SES} \xrightarrow{k_{cat2}} \mathrm{SE} + \mathrm{P} \\ &\mathrm{SE} + \mathrm{S} \underset{k_{43}}{\overset{k_{34}}{\rightleftharpoons}} \mathrm{SES} \end{aligned} \tag{11}$$

In the case when catalytic activity in the SES state is impaired $k_{cat2} \ll k_{cat1}$, the reaction rate decreases with increase in substrate concentration [S] (cf. the Appendix).

Our results suggest an alternative way to achieve the same effect—slow conformational dynamics of the enzyme−substrate complex. The effect does not require allosteric regulation via binding of a second molecule of substrate to the catalytic complex. It appears that the macroscopic kinetic laws resulting from either of the two mechanisms are similar but the mechanisms may be distinguished based on the single-molecule kinetic assessment, i.e. from the waiting time distribution of the successive events. To address this question, one needs an approximation to analytically compute and compare waiting time distributions for schemes describing these two mechanisms. Such calculations can be preformed within a formalism assuming discrete conformational states[13−15] and are discussed in the Appendix. The results indicate that the distribution of catalytic events will be distinct between two mechanisms at saturating substrate concentrations ([S] → ∞).

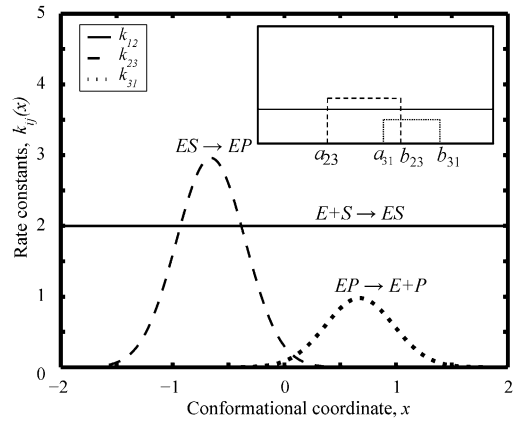

Figure 1. Rate constants $k_{ij}(x)$ as function of the conformational coordinate x, $k_{12} = 2$, $k_BT = 1$, and other values taken from Tables 1 and 2. The inset is a schematic representation of the model rate constants used for the analytical calculation; the analytical expression is derived using the same ordering of boundaries as in the inset.

To understand the origin of substrate inhibition in our kinetic scheme, one needs to focus in Figure 1, which indicates the ranges of conformational coordinates where transitions between the different states are most likely to occur. The product release step from the EP complex EP → E + P takes place along the positive values of x (rate k_{31}, dotted line). The regenerated enzyme E then combines with the free substrate S to form the ES complex. The catalytic step ES → EP takes place along the negative values of x (rate k_{23}, dashed line). At low and intermediate substrate concentrations, the free enzyme has time to diffuse to negative x conformation before binding to the substrate S to form the ES complex; as a result, the catalytic transformation can happen right after substrate binding. At high substrate concentration, the free enzyme regenerated after the product release step (EP → E + P) quickly binds to the substrate to form the ES complex along the positive values of x. Thus the ES complex needs to relax and change its conformation into the negative region of x for the catalytic reaction to take place. However, since conformational dynamics in the ES state is very slow, the most likely way to achieve this conformation is to dissociate the substrate, undergo a conformational change in the E state and then rebind to S in the appropriate conformation. But as the substrate concentration is increased, the time spent in the E state is decreased, effectively slowing down ES relaxation and hence the rate of product formation. Thus the substrate inhibition effect in our model happens because in high substrate concentration the slow conformational diffusion in ES state becomes a rate limiting step. The effect disappears with increases in D_{ES}, as relaxation though S dissociation is no longer required (see Figure 2a, dashed lines). The described mechanism is analogous to the recovery model[23] in which there exists a catalytic cycle in the refractory state which is further locked in this state by substrate binding.

3.2. Analytically Solvable Model. To confirm the results of our numerical simulations, we have also developed an analytically tractable model demonstrating the substrate inhibition effect with the use of a decoupling approximation method proposed by Gopich and Szabo.[15] For simplicity, we chose all potentials to be the same $U_E(x) = U_{ES}(x) = U_{EP}(x) \equiv U(x)$. In that case, generalizing ref 15, we obtain

$$v = \frac{[S]\int dx \frac{k_{23}(x)k_{12}(x)k_{31}(x)}{k_{21}(x)(k_{32}(x)+k_{31}(x))+k_{23}(x)k_{31}(x)+k_{12}(x)[S](k_{23}(x)+k_{32}(x)+k_{31}(x))} e^{-\beta U(x)}}{D_E P_E^0(x)+D_{ES}P_{ES}^0(x)+D_{EP}P_{EP}^0(x)}}{\int dx \frac{e^{-\beta U(x)}}{D_E P_E^0(x)+D_{ES}P_{ES}^0(x)+D_{EP}P_{EP}^0(x)}[S]} \quad (12)$$

$p_i^0(x)$ (i = E, ES, EP) is the local steady state probability of each state for a fixed value of the conformational coordinate x, can be obtained by solving eqs 5 without diffusion terms ($L_i p_i = 0$), and should satisfy the condition $\sum_i p_i^0(x) = 1$. To further simplify this expression in order to obtain an algebraic expression for the reaction rate, we chose $U(x) = 0$ and k_{23}, k_{32}, and k_{31} to be step functions

$$k_{ij}(x) = k_{ij}^0[\theta(x - a_{ij}) - \theta(x - b_{ij})](ij = 23, 32, \text{or } 31) \quad (13)$$

where θ is the Heaviside step function.

A schematic representation of these model rate constants is shown in the inset of Figure 1. These simplified rate constants and potentials allow analytical calculation of the enzyme turnover rate which is given by

$$v = \frac{(b_{23}-a_{31})k_{12}^0k_{23}^0k_{31}^0[S]/(D_E(k_{21}^0k_{32}^0+k_{21}^0k_{31}^0+k_{23}^0k_{31}^0)+D_{ES}[S]k_{12}^0(k_{32}^0+k_{31}^0)+D_{EP}[S]k_{12}^0k_{23}^0)}{\frac{(a_{31}-a_{23})(k_{21}k_{32}+k_{12}[S](k_{23}+k_{32}))}{D_E k_{21}^0k_{32}^0+D_{EP}[S]k_{12}^0k_{23}^0+D_{ES}[S]k_{12}^0k_{32}^0}+\frac{(b_{23}-a_{31})(k_{21}^0k_{32}^0+k_{21}^0k_{31}^0+k_{23}^0k_{31}^0+k_{12}^0[S](k_{23}^0+k_{32}^0+k_{31}^0))}{D_E(k_{21}^0k_{32}^0+k_{21}^0k_{31}^0+k_{23}^0k_{31}^0)+D_{ES}[S]k_{12}^0(k_{32}^0+k_{31}^0)+D_{EP}[S]k_{12}^0k_{23}^0}+\frac{(b_{31}-b_{23})(k_{21}^0k_{31}^0+[S]k_{12}^0k_{31}^0)}{D_E k_{21}^0k_{31}^0+[S]D_{ES}k_{12}^0k_{31}^0}} \quad (14)$$

Figure 2b shows a comparison between the analytically and numerically calculated enzyme turnover rate v as a function of substrate concentration [S] with a sample choice of parameter values (see figure caption for further details). Notably, at large substrate concentrations, the results predicted by eq 5a would be different from the formal quasi-static limit given by $D_{ES} = 0$ (dotted line). From the functional form of eq 14, one can conclude that expansion near $D_{ES} = 0$ will diverge as [S] increases. Notably, the limit $[S] \to \infty$ will result in a finite nonzero rate when $D_{ES} \neq 0$ but will lead to $v = 0$ if $D_{ES} = 0$. From eq 14, one can derive an analytical condition on the diffusion coefficients to allow for the substrate inhibition at high [S]. To do so, we look for parameters that satisfy the inequality $(dv/d[S])|_{[S]\to\infty} \geq 0$. Using a simplified form of eq 14 with $D_E = D_{EP}$ and $k_{32} = 0$, we obtain

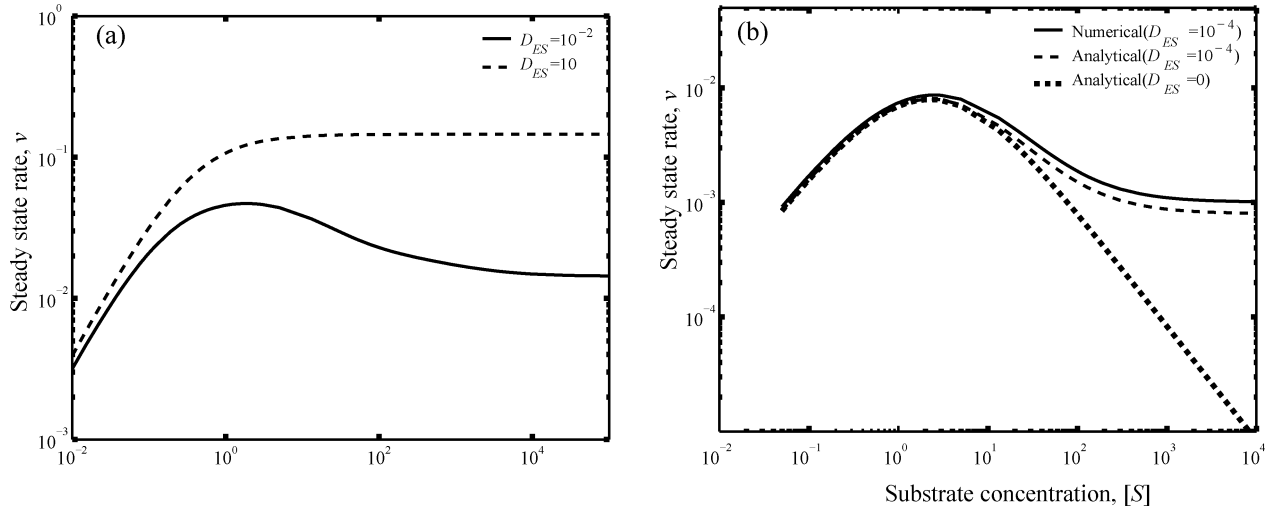

Figure 2. Rate law resulting from slow conformational diffusion. (a) Slow diffusion in ES conformation, $D_{ES} = 10^{-2}$ (open circles), leads to a substrate inhibition effect. The rate approximates Michaelis−Menten for fast diffusion. We used $D_E = D_{EP} = 10$, and the remaining parameter values are taken from Tables 1 and 2. (b) Analytically solvable model confirming substrate inhibition effect and showing the divergence of quasi-static limit at high substrate concentration. Numerical results (solid line) are in good agreement with analytical results (dashed line) calculated with eq 5a for $D_{ES} = 10^{-4}$. Note that regardless of the value of the diffusion coefficient, the solution will deviate from the limit $D_{ES} = 0$ (dotted line) at large substrate concentrations. We used $U = 0$ and stepwise rate constants with $a_{23} = -1.5$, $b_{23} = 0.3$, $a_{31} = 0.1$, $b_{31} = 1.5$, $k_{12}^0 = k_{21}^0 = 1.0$, $k_{23}^0 = k_{32}^0 = 1.5$, and $k_{31}^0 = 0.5$.

$$D_E^2 \geq D_{ES}^2\left(\frac{k_{31}^0}{k_{23}^0} + \frac{(b_{23} - a_{23})}{(b_{31} - b_{23})}\left(\frac{k_{31}^0}{k_{21}^0} + \frac{k_{31}^0}{k_{23}^0}\right)\right) + D_E D_{ES}\left(1 + \frac{k_{31}^0}{k_{21}^0}\right) \quad (15)$$

Note that this condition will be always satisfied if D_{ES} is sufficiently small. Decreases in the product dissociation rate k_{31} or increases in the substrate dissociation rate k_{21} or the catalytic rate k_{23} will extend the range of D_{ES} for which the effect is possible. However, eq 15 is never satisfied when $D_E = D_{ES}$. Thus when diffusion in all three states is very slow, the rate will always monotonically increase with substrate concentration even though our numerical simulations demonstrate the deviation from MM kinetics in this case (not shown). Moreover, inequality 15 cannot be satisfied with the decrease in the conformational region in which substrate is released but catalytic process cannot take place, i.e. as $b_{31} \rightarrow b_{23}$.

3.3. Dynamic Disorder-Driven Bistability. Notably, in the open system with constant supply of substrate and removal of product, substrate inhibition can also lead to multistability (coexistence between several steady states for the same parameter values). Bistability has been experimentally observed in several biochemical systems with substrate inhibition.[24,25] Theoretical analysis[26,27] of such experimental observations suggest that such phenomena arise due to nonlinearity of rate equations which may be a consequence of either substrate inhibition[23] or activation of enzyme reaction by reaction product (positive feedback).[28] To demonstrate the effect of bistability in our case and avoid physically unrealistic infinite substrate accumulation, we introduce a small enzyme-independent leak, $S \rightarrow 0$ with the rate $k_0[S]$. In this case, the steady state of the system is given by the equation

$$\frac{d[S]}{dt} = v_{prod} - v - k_0[S] = 0 \quad (16)$$

where v_{prod} is rate of supply of the substrate and enzymatic rate v is a function of [S] given by eq 8 and shown in Figure 2a.

Figure 3 shows the computed steady state substrate concentrations [S] as a function of supply rate v_{prod}. Within a certain range of values of v_{prod} there exist three steady states, one unstable (U) and two stable (S_1 and S_2). In ref 27, Craciun et al. provide an understanding about the relationship between the structure of mass action biochemical reactions and their capacity to give rise to bistability. They present a theorem that give the conditions and structural requirements an enzyme driven reaction network must meet such that there exist two stable steady states. The theorem is based on reaction networks governed by mass action kinetics and does not predict bistability for the network scheme we used. Therefore, both substrate inhibition and bistability are consequences of deviations from mass-action kinetics caused by dynamic disorder.

4. Conclusions

In summary, we have shown that in the quasi-static limit, even an extremely simplified kinetic scheme can lead not only to a deviation from the classical MM mechanism, but also to inhibition of enzyme activity at high substrate concentration. To corroborate to our numerical results, we used a simplified version of our model to derive an analytical expression of the enzyme turnover rate demonstrating the phenomenon of substrate inhibition. Our model also provides theoretical evidence that dynamic disorder can lead to bistability in a simple reaction network. Moreover, our results point out a general inapplicability of macroscopic rate laws (such as the Michaelis−Menten law) for other kinds of enzymatic reactions in which enzyme exists in more than two states even with a quasi-static limit. For the cases in which conformational dynamics becomes rate limiting in the enzyme−substrate complex, one may expect to see substrate inhibition effects.

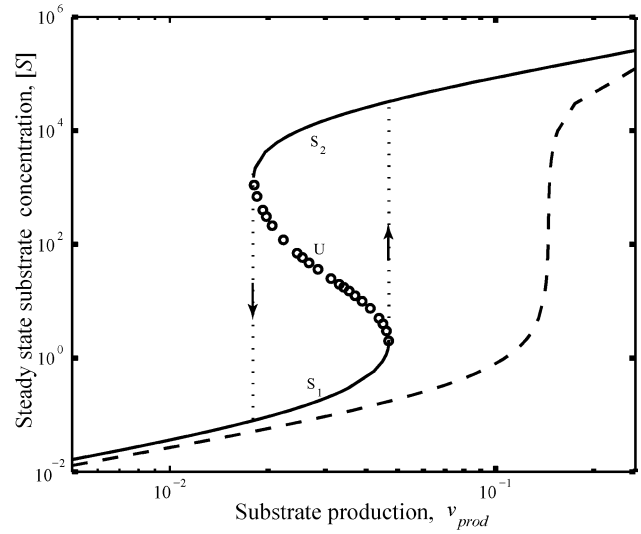

Figure 3. Plot of [S] versus v_{prod} with $k_0 = 10^{-6}$. Bistability at $D_{ES} = 10^{-2}$ and $D_E = D_{EP} = 10$. S_1 and S_2 refer to the stable states, and U is the unstable state. Bistability disappears at $D_{ES} = 10$ (dotted lines). The curves were at the same parameter values used for Figure 2a.

Acknowledgment. The authors are grateful to Jinghua Xing for discussions and providing his Matlab code used in ref 21. The research is supported by a startup fund from Rice University to O.A.I.

Appendix: Finite State Models for Allosteric Regulation and Conformations Dynamics Influenced Substrate Inhibition

In the main text, we have considered effects of conformational fluctuations on the macroscopic rate law and showed it to exhibit substrate inhibition. Here, we compare both macroscopic and single-molecule kinetic descriptions of substrate inhibition and compare these with the case of allosteric substrate inhibition. To simplify the algebra and obtain closed-form analytical expression for single-molecule waiting time distribution, we chose to describe conformational fluctuations with a discrete conformational states model.[13−15]

For simplicity we consider two states of enzyme E_1 and E_2, where only the former exhibits catalytic activity (negative x in continuous description, Figure 1). Product release on the other hand can only happen in the E_2 state (positive x in continuous description, Figure 1). For simplicity, we chose to combine these two reactions resulting in effective reaction

$$ES_1 \xrightarrow{k_{cat}} E_2 + P$$

The full kinetic scheme describing discrete-state approximation of the continuous formalism used in the main text is given by the following reaction scheme:

$$\begin{aligned} &E_1 + S \underset{k_{21a}}{\overset{k_{12a}}{\rightleftharpoons}} ES_1 \xrightarrow{k_{cat}} E_2 + P \\ &E_2 + S \underset{k_{21b}}{\overset{k_{12b}}{\rightleftharpoons}} ES_2 \\ &E_1 \underset{a_2}{\overset{a_1}{\rightleftharpoons}} E_2 \quad ES_1 \underset{b_2}{\overset{b_1}{\rightleftharpoons}} ES_2 \end{aligned} \tag{A.1}$$

The steady state rate can be easily show to be of the form

$$v_{cd} = \frac{A[S] + B[S]^2}{D + E[S] + [S]^2} \tag{A.2}$$

where A, B, D, and E are different combinations of the rate constants k_{12a}, k_{21a}, k_{12b}, k_{21b}, a_1, a_2, b_1, b_2, and k_{cat}. Using suitable values of A, B, D, and E, one can get a reasonably good fit between the discrete-state model rate v_{cd} and the rate computed numerically from eq 8 of the continuous model (see Figure A.1).

Similar substrate inhibition effect can also be obtained from allosteric regulation when a second molecule of substrate binds to allosteric site of the enzyme partially impairing its catalytic activity as described by scheme in eq 11. For this scheme, the steady state rate is given by

$$v_{all} = \frac{A'[S] + B'[S]^2 + C'[S]^3}{D' + E'[S] + F' + [S]^3} \tag{A.3}$$

where A', B', C', D', E', and F' are different combinations of the rate constants k_{12}, k_{21}, k_{13}, k_{31}, k_{24}, k_{42}, k_{34}, k_{43}, k_{cat1}, and k_{cat2}. Despite different functional form of this expression, it is unlikely this difference would be easily detectable as using suitable values of A', B', D', E', E', and F' one can get a very good fit between v_{all} and v_{cd} (see Figure A.1). Thus, the macroscopic rate laws resulting from either of these two mechanisms are practically very similar.

It is interesting to examine, whether these two mechanisms are similar at the microscopic level. Such an analysis can be made from typical single-molecular measurements such as calculating the waiting time distribution between successive catalytic events for both of these mechanisms. In ref 15, Gopich and Szabo proposed a formalism for calculating the statistics of monitored transitions for a given kinetic scheme. A similar type of formalism was presented by Cao[13] to calculate the distribution of time between transitions and the corresponding correlation functions and was used to analyze results from single molecule enzymatic measurements by Lu et al.[7]

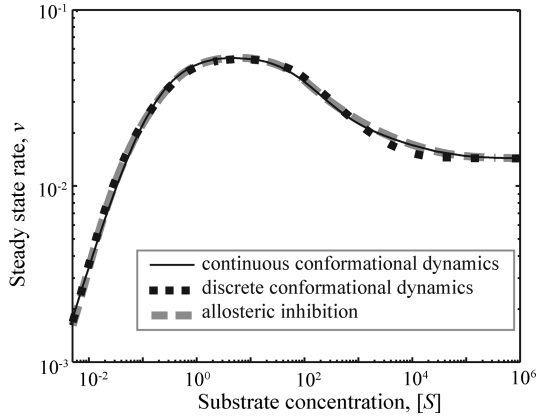

Figure A.1. Comparison of the steady state rate calculated numerically at $D_{ES} = 10^{-2}$ at the same parameter values used for Figure 2a (solid line) with two discrete models, conformational dynamics rate v_{cd} (black dotted line) defined by eq A.2 and allosteric inhibition rate v_{all} (gray dashed line) defined by eq A.3. The parameters are obtained by least-mean square fit of the functional expressions in eqs A.2 and A.3 to the results of numerical simulations from Figure 2a. The resulting parameters are $A = 10.77$, $B = 0.014\,33$, $D = 30.36$, $E = 195.8$, $A' = 5.88 \times 10^4$, $B' = 171.9$, $C' = 0.01433$, $D' = 1.74 \times 10^5$, $E' = 1.038 \times 10^6$, and $F' = 8628$.

Here we calculate the waiting time distribution starting from the formalism proposed by Gopich and Szabo. Let g_i be the probability that the system is in the state i at time t without making a monitored transition. The vector for these probabilities $\vec{g}$ satisfies

$$\frac{d}{dt}\vec{g} = (\mathbf{K} - \mathbf{V})\vec{g} \tag{A.4}$$

where $\mathbf{K}$ is the rate matrix that describes all transitions and $\mathbf{V}$ is the matrix of the monitored (catalytic) transitions only. Following the method shown in ref 15, one can get an expression for the distribution of time between two consecutive monitored transitions which is given by

$$P(t) = \vec{1}^T \mathbf{V} \vec{g}(t) \tag{A.5}$$

where $\vec{1}$ is the unit vector and T denotes transpose. We can apply this formalism to enzymatic reactions presented in schemes eqs 11 and A.1.

For the scheme of eq 11, the matrix $\mathbf{K}$ in the basis (E, ES, SE, SES) is

$$\mathbf{K} = \begin{pmatrix} -(k_{12}[S] + k_{13}[S]) & k_{21} + k_{cat1} & k_{31} & 0 \\ k_{12}[S] & -(k_{21} + k_{cat1} + k_{24}[S]) & 0 & k_{42} \\ k_{13}[S] & 0 & -(k_{34}[S] + k_{31}) & (k_{43} + k_{cat2}) \\ 0 & k_{24}[S] & k_{34}[S] & -(k_{43} + k_{cat2} + k_{42}) \end{pmatrix} \tag{A.6}$$

and the matrix $\mathbf{V}$ is

$$\mathbf{V} = \begin{pmatrix} 0 & k_{cat1} & 0 & 0 \\ 0 & 0 & 0 & 0 \\ 0 & 0 & 0 & k_{cat2} \\ 0 & 0 & 0 & 0 \end{pmatrix} \tag{A.7}$$

Using these $\mathbf{K}$ and $\mathbf{V}$ matrices in eqs A.6 and A.7, we obtain

$$\frac{dg_E}{dt} = -(k_{12}[S] + k_{13}[S])g_E + k_{21}g_{ES} + k_{31}g_{SE} \tag{A.8a}$$

$$\frac{dg_{ES}}{dt} = k_{12}[S]g_E - (k_{21} + k_{cat1} + k_{24}[S])g_{ES} + k_{42}g_{SES} \tag{A.8b}$$

$$\frac{dg_{SE}}{dt} = k_{13}[S]g_E - (k_{34}[S] + k_{31})g_{SE} + k_{43}g_{SES} \tag{A.8c}$$

$$\frac{dg_{SES}}{dt} = k_{24}[S]g_{ES} + k_{34}[S]g_{SE} - (k_{43} + k_{cat2} + k_{42})g_{SES} \quad (A.8d)$$

and

$$P(t) = k_{cat1}g_{ES}(t) + k_{cat2}g_{SES}(t) \quad (A.9)$$

Solving these equations in the Laplace space with proper initial conditions we can obtain analytical expression for $\hat{P}(s) = k_{cat1}\hat{g}_{ES}(s) + k_{cat2}\hat{g}_{SES}(s)$. The Laplace transform can be easily inverted at the limit of saturating substrate concentration ([S] $\rightarrow \infty$) and result in an exponential waiting time distribution

$$P(t) = k_{cat2}e^{-k_{cat2}t} \quad (A.10)$$

The mean waiting time $\tau = \int_0^\infty tf(t)\,dt$ is given by

$$\tau = \frac{1}{k_{cat2}} \quad (A.11)$$

Similar calculations can be performed for the scheme A.1. For this system, the matrix **K** in the basis (E_1, E_2, ES_1, ES_2) is given by

$$\mathbf{K} = \begin{pmatrix} -(k_{12a}[S] + a_1) & a_2 & k_{21a} & 0 \\ a_1 & -(k_{12b}[S] + a_2) & k_{cat} & k_{21b} \\ k_{12a}[S] & 0 & -(k_{21a} + k_{cat} + b_1) & b_2 \\ 0 & k_{12b}[S] & b_1 & -(k_{21b} + b_2) \end{pmatrix} \quad (A.12)$$

and the matrix **V** is given by

$$\mathbf{V} = \begin{pmatrix} 0 & 0 & 0 & 0 \\ 0 & 0 & k_{cat} & 0 \\ 0 & 0 & 0 & 0 \\ 0 & 0 & 0 & 0 \end{pmatrix} \quad (A.13)$$

Using these **K** and **V** matrices in eqs A.12 and A.13, we obtain

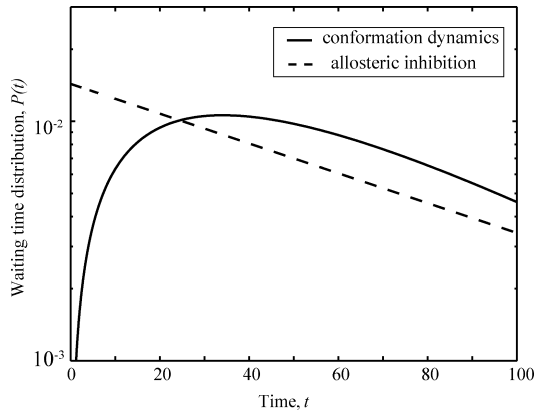

Figure A.2. Comparison of the waiting time distributions calculated at saturating substrate concentration [S] $\rightarrow \infty$ for the mechanism of allosteric inhibition (dashed line) with the one describing slow conformational dynamics (solid line). The parameters $k_{cat2} = 0.014\,33$, $k_{cat} = 0.025$, $b_1 = 0.033\,957$, and $b_2 = 0.034$ are chosen to produce the identical mean waiting times that correspond to reaction rate as in Figure A.1 at [S] $\rightarrow \infty$.

$$\frac{dg_{E_1}}{dt} = -(k_{12a}[S] + a_1)g_{E_1} + a_2g_{E_2} + k_{21}g_{ES_1} \quad (A.14a)$$

$$\frac{dg_{E_2}}{dt} = a_1g_{E_1} - (a_2 + k_{12b}[S])g_{E_2} + k_{21b}g_{ES_1} \quad (A.14b)$$

$$\frac{dg_{ES_1}}{dt} = k_{12a}[S]g_{E_1} - (k_{21a} + k_{23} + b_1)g_{ES_1} + b_2g_{ES_2} \quad (A.14c)$$

$$\frac{dg_{ES_2}}{dt} = k_{12b}[S]g_{E_2} + b_1g_{ES_1} - (k_{21b} + b_2)g_{ES_2} \quad (A.14d)$$

and

$$P(t) = k_{cat}g_{ES_1}(t) \quad (A.15)$$

Solving eqs A.14 in the Laplace space and using it in $\hat{P}(s) = k_{cat}\hat{g}_{ES_1}(s)$, we can again obtain an algebraic expression for Laplace transform of waiting time distribution. Inverse Laplace at the limit of saturating substrate concentration ([S] $\rightarrow \infty$) results in

$$P(t) = k_{cat}b_2\frac{e^{-(b_1+b_2+k_{cat}-\kappa)t/2} - e^{-(b_1+b_2+k_{cat}+\kappa)t/2}}{\kappa},$$
$$\text{where } \kappa = \sqrt{(b_1 + b_2 + k_{cat})^2 - 4b_2k_{cat}} \quad (A.16)$$

The mean waiting time is given by

$$\tau = \frac{b_1 + b_2 + k_{23}}{b_2k_{cat}} \quad (A.17)$$

Thus the distribution of time between consecutive catalytic turnovers at infinite substrate concentration is a mono-exponential decay for true allosteric regulation and a difference of two exponentials for the case of substrate inhibition modulated by slow conformational fluctuations. Figure A.2 gives a comparison of the waiting time distributions for these two mechanisms. The parameters chosen gave the same mean waiting time (the reciprocal of which is the rate) for both of the schemes. Thus, microscopically these two mechanisms are different though they behave quite similar macroscopically.

References and Notes

(1) Michaelis, L.; Menten, M. L. *Biochem. Z.* **1913**, *49*, 333.
(2) (a) Fersht, A. *Enzyme Structure and Mechanism*; Academic: New York, 1982. (b) Segel, I. H. *Enzyme Kinetics: Behavior and Analysis of Rapid Equilibrium and Steady-State Enzyme Systems*; Wiley: New York, 1993.
(3) Yon, J. M.; Perahia, D.; Ghelis, C. *Biochimie* **1998**, *80*, 33.
(4) Hammes, G. G. *Biochemistry* **2002**, *41*, 8221.
(5) Hammes-Schiffer, S.; Benkovic, S. J. *Annu. Rev. Biochem.* **2006**, *75*, 519.
(6) (a) Monod, J.; Wyman, J.; Changeux, J. P. *J. Mol. Biol.* **1965**, *12*, 88. (b) Koshland, D. E.; Nemethy, G.; Filmer, D. *Biochemistry* **1966**, *5*, 365. (c) Weber, G. *Biochemistry* **1972**, *11*, 864. (d) Kern, D.; Zuiderweg, E. R. P. *Curr. Opin. Struct. Biol.* **2003**, *13*, 748.

(7) Lu, H. P.; Xun, L.; Xie, X. S. *Science* **1998**, *282*, 1877.
(8) Yang, H.; Luo, G.; Karnchanaphanurach, P.; Louie, T.-M.; Rech, I.; Cova, S.; Xun, L.; Xie, X. S. *Science* **2003**, *302*, 262.
(9) (a) Kou, S. C.; Xie, X. S. *Phys. Rev. Lett.* **2004**, *93*, 180603. (b) Min, W.; Luo, G.; Cherayil, B. J.; Kou, S. C.; Xie, X. S. *Phys. Rev. Lett.* **2005**, *94*, 198302.
(10) (a) Eisenmesser, E. Z.; Bosco, D. A.; Akke, M.; Kern, D. *Science* **2002**, *295*, 1520. (b) Palmer, A. G. *Chem. Rev.* **2004**, *104*, 3623. (c) Eisenmesser, E. Z.; Millet, O.; Labeikovsky, W.; Korzhnev, D. M.; Wolf-Watz, M.; Bosco, D. A.; Skalicky, J. J.; Kay, L. E.; Kern, D. *Nature* **2005**, *438*, 117. (d) Henzler-Wildman, K. A.; Thai, V.; Lei, M.; Ott, M.; Wolf-Watz, M.; Fenn, T.; Pozharski, E.; Wilson, M. A.; Petsko, G. A.; Karplus, M.; Hübner, C. G.; Kern, D. *Nature* **2007**, *450*, 838.
(11) English, B. P.; Min, W.; van Oijen, A. M.; Lee, K. T.; Luo, G.; Sun, H.; Cherayil, B. J.; Kou, S. C.; Xie, X. S. *Nat. Chem. Biol.* **2006**, *2*, 87.
(12) (a) Zwanzig, R. *Acc. Chem. Res.* **1990**, *23*, 148. (b) Zwanzig, R. *J. Chem. Phys.* **1992**, *97*, 3587.
(13) (a) Cao, J. *Chem. Phys. Lett.* **2000**, *327*, 38. (b) Yang, S.; Cao, J. *J. Chem. Phys.* **2002**, *117*, 10996.
(14) Kou, S. C.; Cherayil, B. J.; Min, W.; English, B. P.; Xie, X. S. *J. Phys. Chem. B* **2005**, *109*, 19068.
(15) Gopich, I. V.; Szabo, A. *J. Chem. Phys.* **2006**, *124*, 154712.
(16) Min, W.; Gopich, I. V.; English, B. P.; Kou, S. C.; Xie, X. S.; Szabo, A. *J. Phys. Chem. B* **2006**, *110*, 20093.
(17) Xue, X.; Liu, F.; Ou-Yang, Z. C. *Phys. Rev. E* **2006**, *74*, 030902(R).
(18) Chaudhury, S.; Cherayil, B. J. *J. Chem. Phys.* **2007**, *127*, 105103.
(19) Agmon, N.; Hopfield, J, J. *J. Chem. Phys.* **1983**, *78*, 6947.
(20) Wang, H.; Peskin, C.; Elston, T. *J. Theor. Biol.* **2003**, *221*, 491.
(21) Xing, J. *Phys. Rev. Lett.* **2007**, *99*, 168103.
(22) (a) Kuhm-Velten, W. N.; Bunse, T.; Forster, M. E. C. *J. Biol. Chem.* **1991**, *266*, 6291. (b) Shen, P.; Larter, R. *Biophys. J.* **1994**, *67*, 1414. (c) Collom, S. L.; Laddusaw, R. M.; Burch, A. M.; Kuzmic, P.; Perry, Jr. M. D.; Miller, G. P. *J. Biol. Chem.* **2008**, *283*, 3487.
(23) Kuhl, P. W. *Biochem. J.* **1994**, *298*, 171.
(24) Degn, H. *Nature* **1968**, *217*, 1047.
(25) (a) Geiseler, W.; Föllner, H. H. *Biophys. Chem.* **1977**, *6*, 107. (b) Frenzel, J.; Schellenberger, W.; Eschrich, K. *Biol. Chem. Hoppe-Seyler* **1995**, *376*, 17.
(26) (a) Edelstein, B. B. *J. Theor. Biol.* **1970**, *29*, 57. (b) Hervagault, J. F.; Canu, S. *J. Theor. Biol.* **1987**, *127*, 439. (c) Gray, P.; Scott, S. K. In *Chemical Oscillations and Bistability*; Clarendon Press: Oxford, 1994. (d) Guidi, G. M.; Carlier, M. F.; Goldbeter, A. *Biophys. J.* **1998**, *74*, 1229.
(27) Craciun, J.; Tang, Y.; Feinberg, M. *Proc. Natl. Acad. Sci. U.S.A.* **2006**, *103*, 8697.
(28) (a) Xiong, W.; Ferrell, J. E., Jr. *Nature* **2003**, *426*, 460. (b) Angeli, D.; Ferrell, J. E., Jr.; Sontag, E. D. *Proc. Natl. Acad. Sci. U.S.A.* **2004**, *101*, 1822. (c) Maamar, H.; Dubnau, D. *Mol. Microbiol.* **2005**, *56*, 615.

JP907908D